Virus Research 274 (2019) 197778

Contents lists available at ScienceDirect

Virus Research

journal homepage: www.elsevier.com/locate/virusres

A novel molecular mechanism to explain mutations of the HCV protease associated with resistance against covalently bound inhibitors

Leonardo Nazario de Moraes[a], Rejane Maria Tommasini Grotto[a,b], Guilherme Targino Valente[a,c], Heloisa de Carvalho Sampaio[b], Angelo José Magro[a,b,d], Lauana Fogaça[a,d], Ivan Rodrigo Wolf[d], David Perahia[e], Giovanni Faria Silva[b], Rafael Plana Simões[a,b,*]

[a] Sao Paulo State University (UNESP), School of Agriculture, Department of Bioprocess and Biotechnology, Avenue Universitária, 3780, Botucatu, SP, Brazil
[b] Sao Paulo State University (UNESP), Medical School, Blood Center, Avenue Prof. Mário Rubens Guimarães Montenegro, s/n, Botucatu, SP, Brazil
[c] Max Planck Institut for Heart and Lung Research, Ludwigstraße 43, 61231, Bad Nauheim, Germany
[d] Sao Paulo State University (UNESP), Institute of Biosciences, Street Prof. Dr. Antônio Celso Wagner Zanin, 250, Botucatu, SP, Brazil
[e] École Normale Supérieure Paris-Saclay, Laboratory of Biology and Applied Pharmacology, Cachan, 94235, France

ARTICLE INFO

Keywords:
HCV
Direct-acting antiviral
Boceprevir
Treatment failure
Resistance associated substitutions

ABSTRACT

NS3 is an important therapeutic target for direct-acting antiviral (DAA) drugs. However, many patients treated with DAAs have unsustained virologic response (UVR) due to the high mutation rate of HCV. The aim of this work was to shed some light on the puzzling molecular mechanisms of the virus's of patients who showed high viral loads even under treatment with DAA. Bioinformatics tools, molecular modelling analyses were employed to identify mutations associated with HCV resistance to boceprevir and possible structural features related to this phenomenon. We identified two mutations of NS3 that may be associated with HCV resistance: D168N and L153I. The substitution D168N was previously reported in the literature as related with drug failure. Additionally, we identified that its molecular resistance mechanism can be explained by the destabilization of receptor-ligand hydrogen bonds. For the L153I mutation, the resistance mechanism is different from previous models reported in the literature. The L153I substitution decreases the S139 deprotonation susceptibility, and consequently, this mutation impairs the covalent binding between the residue S139 from NS3 and the electrophilic trap on boceprevir, which can induce drug failure. These results were supported by the time course analysis of the mutations of the NS3 protease, which showed that boceprevir was designed for enzymes with an L residue at position 153; however, the sequences with I153 are predominant nowadays. The results presented here could be used to infer about resistance in others DAA, mainly protease inhibitors.

1. Introduction

Chronic hepatitis C is characterized by a progressive infection caused by the hepatitis C virus (HCV). 7 genotypes (from 1 to 7) and 67 subtypes of HCV have been identified, highlighting the genetic variability of this virus (Halfon and Locarnini, 2011; Simmonds et al., 2005; Smith et al., 2014). In addition, (Borgia et al. (2018)) recently reported the circulation of a newly identified HCV lineage in the Indian subcontinent, which was characterized as genotype 8.

The serine protease NS3 is an HCV enzyme that presents a chymotrypsin-like fold with a C-terminal domain containing a six-stranded β-barrel and an N-terminal domain with eight β-strands (Kim et al., 1996). Separating these two β-barrel domains is a deep crevice that harbours a triad composed of coordinated amino acid residues H57, A81 and S139, which are an essential part of the NS3 catalytic site (Kim et al., 1996). NS3 serine protease is responsible for the cleavage of polyproteins and the release of individual proteins that compose the HCV viral RNA replication machinery (Kim et al., 1996; Penin et al., 2004); therefore, it is an important biological target for antiviral drugs such as boceprevir and telaprevir (Morales and Aguado, 2012).

Boceprevir (a substrate-like inhibitor), combined with Peginterferon alfa-2a and ribavirin, was the first combined therapy with DAA used to chronic hepatitis C treatment, indicated for the treatment of HCV genotype 1-infected chronic patients (Venkatraman, 2012). The chemical kinetics of the boceprevir inhibition mechanism involves two steps: firstly, the stabilization between the inhibitor and NS3 by

* Corresponding author at: Sao Paulo State University (UNESP), School of Agriculture, Department of Bioprocess and Biotechnology, Avenue Universitária, 3780, Botucatu, SP, Brazil.
E-mail address: rafael.simoes@unesp.br (R. Plana Simões).

https://doi.org/10.1016/j.virusres.2019.197778
Received 29 July 2019; Received in revised form 7 October 2019; Accepted 8 October 2019
Available online 13 October 2019
0168-1702/

hydrogen bonds, followed by a second step involving a nucleophilic attack triggering the formation of the covalent and reversible bond (Howe and Venkatraman, 2013). This second step is only possible due to the presence of an electrophilic trap, or 'warhead,' in the boceprevir molecular structure that makes possible the covalent binding of this inhibitor to the NS3 amino acid residue S139, which is part of the conserved catalytic triad of the serine protease.

Regarding therapeutics, NS3 mutations can confer HCV drug resistance since amino acid substitutions potentially affect substrate specificity and/or induced-fit binding. Currently, the literature reports some mutations that can be related to the high HCV resistance to protease inhibitors. (Shiryaev et al. (2012)) have shown that the most common mutations associated with viral resistance in NS3 are V36M, R155K, A156T, D168A and V170A, among which the mutations V36M, R155K, A156T and V170A are related to the reduced sensitivity of boceprevir. (Halfon and Locarnini (2011)) also identified the following mutations associated with boceprevir resistance in HCV: V36A/M, T54A, V55A, V70A, R155K/T/Q and A156V/T/S. Additionally, (Coppola et al. (2016)) listed new mutations associated with boceprevir resistance, such as V36L, T54S, V107I, R155C, V158I and D168N. Recently, the NS3 variant 174H was identified as potentially related to the protease inhibitors (PI) resistance, without any explanation of the molecular mechanisms of the resistance (Cuypers et al., 2017).

The understanding of HCV genotypic drug resistance remains a challenge, especially in patients who previously failed under direct-acting antiviral DAA therapy and need to be retreated with a second DAA-based regimen. Given the importance of HCV resistance against antiviral drugs, we analysed plasma samples from chronic hepatitis C patients to detect NS3 mutations related to boceprevir resistance and identified new amino acid substitutions associated with this viral phenotype. Moreover, based on molecular dynamics simulations and quantum mechanics features, we also proposed a novel molecular mechanism that could explain the structural basis of boceprevir resistance induced by a specific kind of mutation.

2. Materials and methods

2.1. Experimental group

Plasma samples were collected from 31 chronic hepatitis C patients infected with genotype 1 HCV under medical supervision at the Hepato-Hemocenter Outpatient Clinic of the Medical School Clinics Hospital, UNESP, Botucatu/SP, Brazil. All patients included in this study were under regular treatment with the protease inhibitor boceprevir. Out of this experimental group, 22 did not have a sustained virologic response (no SVR) and 9 presented with a sustained virologic response (SVR). Patients younger than 18-years-old, pregnant women, patients coinfected with other viruses, or patients with any other pathology of hepatic aetiology were not included in the experimental group. This study was approved by the Research Ethics Committee of Botucatu Medical School, UNESP (Document number 1.440.367). Written informed consent was obtained from each patient included in the study. The study protocol conforms to the ethical guidelines of the 1975 Declaration of Helsinki as reflected in a priori approval by the institution's human research committee.

2.2. Molecular biology analyses

Viral RNA extractions were performed from frozen plasma using the QIAamp® Viral RNA Mini Kit (Qiagen, USA) following the manufacturer's instructions. The cDNA synthesis was performed in a 20 µL reaction using a High-Capacity cDNA Reverse Transcription Kit (ThermoFisher, USA). Ten microliters of extracted RNA were added in 1X RT Buffer, 10 mM dNTPs, 1X random primers and 50 U MultiScribe™ Reverse Transcriptase. The cDNA reaction was incubated at 25 °C for 10 min, 37 °C for 2 h and then at 85 °C for 5 min. The amplification of the NS3 region was performed in two steps. First-round PCR was carried out with 5 µL of cDNA, 0.2 µM of each specific primer to NS3 (F1 5′-GAR CCM GTC GTC TTC TCC-3′ and R1 5′-TGG TGG ACA GAG CRA CCT CCT-3′), 1 X PCR buffer, 1.5 mM $MgCl_2$, 0.5 mM dNTPs and 0.5 U Platinum™ Taq DNA Polymerase High Fidelity (ThermoFisher, USA) in a 25 µL reaction. The amplification was carried out at 94 °C for 5 min, followed by 35 cycles at 94 °C for 30 s, 54 °C for 30 s, 72 °C for 1 min, and final extension at 94 °C for 5 min. The second step (Nested-PCR) was performed using the same protocol as the first-round PCR, except it contained 5 µL of the amplified product in the first-round PCR and NS3 nested primers (F1 5′-GAR CCM GTC GTC TTC TCC-3′ and R2 5′- GGT RGA GTA CGT GAT GGG G-3′). Nested-PCR amplified products were loaded into a 1% agarose gel electrophoresis assay and the band corresponding to the NS3 region was cut out and purified using the Invisorb Fragment CleanUp kit (Invitek, USA) following the manufacturer's instructions. Purified products sequencing was performed using both primers of Nested-PCR and BigDye™ Terminator v3.1 Cycle Sequencing kit (ThermoFisher, USA) on an ABI 3500 DNA analyser (ThermoFisher, USA). Chromatogram quality and forward and reverse sequence merging were performed using Geneious software.

2.3. Inference of mutations of NS3 associated with virus resistance

We performed phylogenetic inference, machine learning and selective pressure analysis to infer the NS3 mutations that may be associated with the virus resistance.

A total of 3,681 sequences of NS3 domains from HCV genotype 1a sequences were downloaded from NCBI; both nucleotides and amino acids were accessed for each sample. Sequences ≤144 aa and those with many ambiguities were deleted and further trimmed based on our patients' sequences. The trimmed sequences were aligned using CLUSTAL OMEGA (Sievers and Higgins, 2014), and miss-aligned sequences were excluded. The CD-HIT (Huang et al., 2010) (identity 1, -G no, -g 1, -b 20, -aL 0.99, and -aS 0.99) were used to reduce redundancies, generating a total of 647 sequences, and these were aligned with the sequences of our patients using MUSCLE (Edgar, 2004). The maximum likelihood tree was inferred using RAXML (Stamatakis, 2014) and implemented at CRIPRES Science Gateway (Miller et al., 2010); this tree allowed us to rank the sequence ACA50657 (for the nucleotide, EU482867) as an out-group to the selective pressure analysis.

The two amino acid sequences from each patient (one before treatment and one after drug failure) were pairwise aligned using MUSCLE (Edgar, 2004), and amino acid (aa) substitutions were listed and checked concerning its selective pressure status in order to identify the sites which are affecting the virus adaptability (or fitness) (Ali et al., 2010). For this purpose, the whole set of nucleotide sequences of our patients and the aforementioned outgroup were aligned using MUSCLE (Edgar, 2004) and submitted to the selective pressure analysis using Datamonkey (Delport et al., 2010). MEME was used to find directed selection, and SLAC was used to find the codons, with both methods using TrN as the evolutionary model (8th best ranked using the JmodelTest with AIC).

The NS3 sequences of HCV from SVR and UVR patients were also used as inputs for the machine learning (ML) analyses in order to find patterns in alignment data. The nucleotides from NS3 sequences were used as attributes and the virologic response of each patient was used as the class (SVR and UVR). Thus, ML analysis was performed to identify if any specific mutation (or a combination of mutations) could be associated with virus resistance against the DAAs (Shen et al., 2016). ML was performed using Weka (Han et al., 2011), applying the J48 algorithm. The robustness of the network was evaluated by the area under the ROC curve (AUC) obtained from the matrix of confusion for the generated model.

The mutations identified as potentially associated with virus resistance obtained by phylogenetic and/or ML analyses were selected for

the subsequent analysis of this study.

2.4. Molecular dynamics simulations

Molecular dynamics (MD) simulations were performed, using the crystallographic structure of the HCV NS3 protease domain complexed with NS4A peptide and boceprevir (PDB ID: 2OC8) (Prongay et al., 2007). Each selected mutation from selective pressure and ML analysis (V36M, Q80K, L153I, and D168N, further discussed) was built in a different NS3/NS4A/boceprevir molecular complex using Charmm software v.36b1 (Vanommeslaeghe et al., 2010; Brooks et al., 2009). The PDB2PQR server (Dolinsky et al., 2004) was used to evaluate the protonation states of the amino acid residues of each structure at pH 7.0. Previous pK_a results described in the literature were also used, especially those presented by Shiryaev et al., which show the NS3 protease presents two Zn^{+2}-coordination sites with three cysteines (C97, C99 and C145) and one histidine (H149). The topology of these modified residues was obtained from (Foloppe et al. (2001)), and the CGenFF (Vanommeslaeghe et al., 2010) server was employed to determine the topology of the boceprevir molecule.

Initially, all structures (each one containing one a specific mutation) were energetically minimized and then submitted to a 100 ps-MD simulation using the Charmm36 force field (Vanommeslaeghe et al., 2010) in the presence of an implicit solvent, followed by steepest descent (SD) and Adopted Basis Newton-Raphson (ABNR)-based energy minimization (500 steps). Next, 100 ns-MD simulations under constant temperature (T = 300 K) and pressure (1.0 bar) were performed, applying the Charmm36 force field with explicit solvent (TIP3P) in a $91 \times 68 \times 73$ Å box. The stability analysis of the NS3/boceprevir complex during the MD simulations were based on the length of the hydrogen bonds between the drug and receptor.

2.5. Reactivity indexes

Analyses of the Condensed-to-atoms Fukui indexes (CAFIs) were performed to verify the viability of the covalent binding between boceprevir and the amino acid S139 from the NS3 protease. The molecular structure of boceprevir that was used for these analyses was obtained from the ChemSpider repository (Boceprevir | C27H45N5O5 | ChemSpider, 2019). The structure of the S139 residue was obtained from the same PDB server previously cited (PDB ID: 2OC8). The covalent bonds between S139 and the other NS3 amino acids were replaced by hydrogen terminals to promote the molecular stabilization during the electron population analyses.

All the molecules were fully optimized via density functional theory (DFT) calculations using Gaussian software (Frisch et al., 2016). Becke's LYP (B3LYP) exchange-correlation functional and 6–31 G(p,d) basic sets were employed. The polarizable continuum model (PCM) was used to simulate the presence of the solvent at this stage.

The evaluation of molecular reactivity was accomplished by CAFIs. The three distinct CAFIs can be defined as:

$$f_k^{+} = q_k\,(N+1) - q_k\,(N) \text{ for nucleophilic attack on atom } k \quad (1)$$

$$f_k^{-} = q_k\,(N) - q_k\,(N-1) \text{ for electrophilic attack on atom } k$$

$$f_k^{0} = \tfrac{1}{2}\,[q_k\,(N+1) - q_k\,(N-1)] \text{ for radical attack on atom } k$$

where $qk\,(N+1)$, $qk\,(N)$ and $qk\,(N-1)$ represent the electronic Hirshfeld population on the *k-th* atom of anionic, cationic and neutral species, respectively, of the studied compound (Cesarino et al., 2016; Donini et al., 2018).

2.6. Molecular clock and temporal analysis of the HCV mutations

For the molecular clock analysis, the nucleotide sequences of the NS3 647 domain, selected as already reported, plus the sequences of our patients were submitted to a phylogenetic inference, followed by a molecular clock calculation. To estimate the molecular clock, the BEAST (Drummond et al., 2012) software in the CIPRES Science Gateway (Miller et al., 2010) was configured to use a starting UPGMA tree topology and the general time reversible (GTR) substitution model with 4 gamma categories plus invariant sites, as well as the uncorrelated relaxed clock model, for 100 million generations. Also, to select the specific mutation sites of NS3, a new CD-HIT was performed and 213 DNA sequences were used with five extra sequences: DQ437509 (genotype 3a), DQ418785 (genotype 4), Y13184 (genotype 5a), DQ278892 (genotype 6), EF108306 (genotype 7a) downloaded from NCBI database as outgroups. The molecular clock tree was visualized with Figtree v1.4.4.

For temporal analysis of the HCV mutations, the nucleotide sequences from NCBI were also used. In addition, all NS3 sequences were obtained from the PDB for which the crystallography structures were docked with any type of VHC inhibitor, resulting in a total of 82 sequences. The sequences were aligned using the same methodology previously described. The inhibitors of each sequence were identified and classified into three possible groups according their interaction with NS3 protease: 1) inhibitors covalently bonded to residue S139 (referred to as 'covalently bonded' in the results section); 2) inhibitors non-covalently bonded to residue S139 (referred to as 'others' in the results section); and 3) inhibitors for which the chemical interactions with NS3 are unknown or not well described in the literature (referred to as 'unknown' in the results section).

3. Results and discussion

3.1. NS3 mutation selections

Sequencing of HCV revealed many mutations in the viral genome isolated from patients that were unresponsive to boceprevir treatment. Fig. 1 presents a map with all NS3 mutations of patients with UVR. A number of those mutations were previously associated with boceprevir resistance, but only a few had their resistance mechanism described in the literature, which are explored in detail later. The resistance mechanism of the new mutations reported here was also explored. The knowledge of possible mechanisms of resistance could lead to a better understanding of the dynamic drug-enzyme interaction applied to other DAAs.

The selective pressure analysis showed the V36M, Q80K, L153I and D168N mutations were neither positively nor negatively selected; thus, we assumed them to be under neutral selection. Despite virus

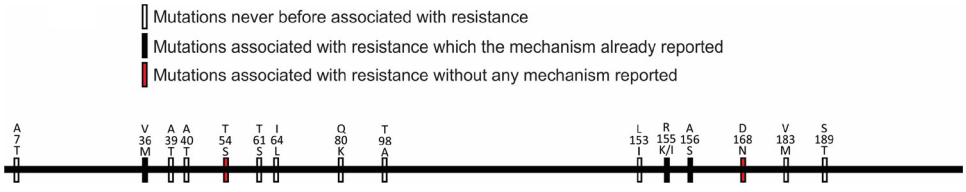

Fig. 1. Map of variations in HCV NS3 protease identified in patients that were unresponsive to boceprevir treatment. The horizontal line represents the amino acid sequence of the NS3 enzyme; the vertical lines and their numbers indicate the position of each observed variant compared to the reference (PDB ID: 2OC8). The empty vertical lines indicate variants not associated with resistance, while the black variants are associated with resistance and the red variants are associated with resistance with the mechanism already described. The first letter on each variant represents the NS3 sequence of the reference, while the last letter indicates the mutation identified here as unresponsive to boceprevir treatment.

experience strong selective forces, most of variations in virus genomes are neutrally fixed in the population (Frost et al., 2018), and some resistances of HCV to protease inhibitors exist in these genomes without any selection prone to these mutations (Sanjuán and Domingo-Calap, 2016). However, it is interesting to note that the V36M and D168N mutations have been previously reported in the literature as being associated with drug resistance; however, only the V36M substitution has had its molecular mechanism elucidated. Thus, the Q80K, L153I and D168N mutations were selected for the molecular dynamics analysis.

Results from machine learning analysis revealed that three mutations may be associated with drug resistance: T98A, R155K and, again, the V36M mutation; the area under the ROC curve (AUC ≈ 0.74) supports this inference. Mutations R155K and V36M were already reported in the literature as being associated with drug resistance. Thus, the T98A mutation was also selected for MD simulations.

Taken together, the mutations Q80K, T98A, L153I and D168N were selected for the MD simulations. For comparative purposes, the simulations were also performed for the A156S mutation, a substitution frequently associated with resistance to boceprevir.

3.2. Molecular modelling analyses

To guide the presentation and discussion of subsequent results, the three-dimensional structure of the boceprevir molecule was referred to, for which only the atoms that will be cited in this paper were identified with labels (Fig. 2a). Fig. 2b shows the drug CAFIs (f^+), which revealed the electrophilic trap of this category of DAA (Venkatraman, 2012; Howe and Venkatraman, 2013).

Table 1 shows the mean of the binding distances (and their respective standard deviations) from MD simulations of hydrogen bonds reported in the literature to stabilize the linker (boceprevir) to the receptor (NS3). The results are shown for the wild type, as well as the A156S and D168N mutations. The enzymes with mutations Q80K, T98A, L153I did not present significant results (data not shown).

All hydrogen bonds between the receptor and the linker were stable in the wild type, i.e., they fluctuated in an acceptable limit for a hydrogen bond. However, the hydrogen bonds are destabilized when the enzyme was A156S and D168N mutated. The result for the A156S substitution was expected, since its molecular resistance mechanism is caused by the destabilization of hydrogen bonds between receptor and linker as previously reported (Halfon and Locarnini, 2011). In addition, here we propose that a D168N mutation results in a resistance mechanism similar to the A156S mutation, which was supported by the results from MD simulations. In fact, the time course analysis of the distance between the NE2 atom (from the amino acid H57) and the O33 atom (from boceprevir) revealed an unstable interaction between receptor and ligand when NS3 was A156S and D168N mutated (Fig. 3).

However, the stability of the hydrogen bonds between the drug and the enzyme did not explain the resistance mechanism concerning the other selected mutations (Q80K, T98A and L153I). This indicates that these mutations may impair the second stage of the chemical reaction that stabilizes the drug at the catalytic site of the protease (the reversible covalent bond between amino acid S139 and atom C28 from the drug). Thus, the results allow for the proposal of a novel mechanism based on the viability of the covalent reaction between the electrophilic trap of the boceprevir and the NS3 catalytic site.

The results from the reactivity indexes showed that the OG from S139 (in its protonated state) is not susceptible to an electrophilic attack (f^-) (Fig. 4a). The deprotonation process on the OG atom of S139 is required to allow the covalent bond to form between the receptor and the ligand. The results also show the OG became the most susceptible

Table 1
Mean and standard deviations of the binding distances of hydrogen bonds to stabilize the linker (boceprevir) to the receptor (NS3). For NS3, the atoms labelled were the same as those utilized in the PDB ID: 2OC8. The * symbol indicates destabilized hydrogen bond.

NS3 residue - atom	Boceprevir atom	Bond lenght (Å)		
		Wild	A156S	D168N
T42 - O	N36	3.37 ± 0.31	2.93 ± 0.22	3.03 ± 0.22
H57 - NE2	O33	3.49 ± 0.29	3.95 ± 0.69*	4.03 ± 0.53*
G137 - N	O35	2.90 ± 0.15	2.87 ± 0.15	3.06 ± 0.22
S139 - N	O35	3.34 ± 0.28	3.50 ± 0.41	3.24 ± 0.38
A157 - N	O15	3.21 ± 0.20	3.17 ± 0.21	3.03 ± 0.16
A157 - O	N3	3.05 ± 0.18	3.25 ± 0.24	3.12 ± 0.20
A157 - O	N8	2.97 ± 0.14	2.99 ± 0.16	2.94 ± 0.14

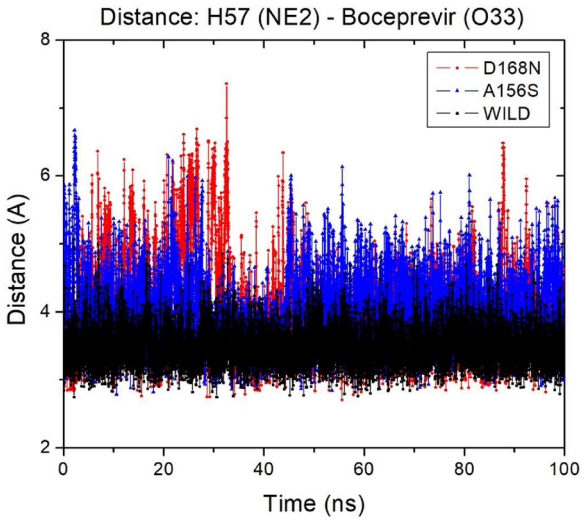

Fig. 3. Distance between the NE2 atom from the H57 residue and the O33 atom from boceprevir in the MD simulations. The results are presented for wild-type NS3, A156S mutated and D168N mutated.

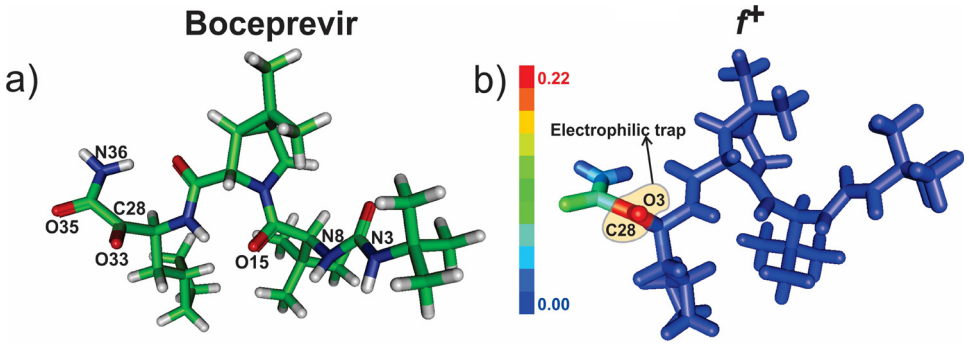

Fig. 2. (a) 3D structure of the boceprevir molecule. The atom colours follow convention: carbon (green), hydrogen (light grey), nitrogen (blue) and oxygen (red). **(b)** CAFIs (f^+) for boceprevir, in which the electrophilic trap is highlighted. f^+ colouration indicates the susceptibility of each atom to suffer a nucleophilic attack.

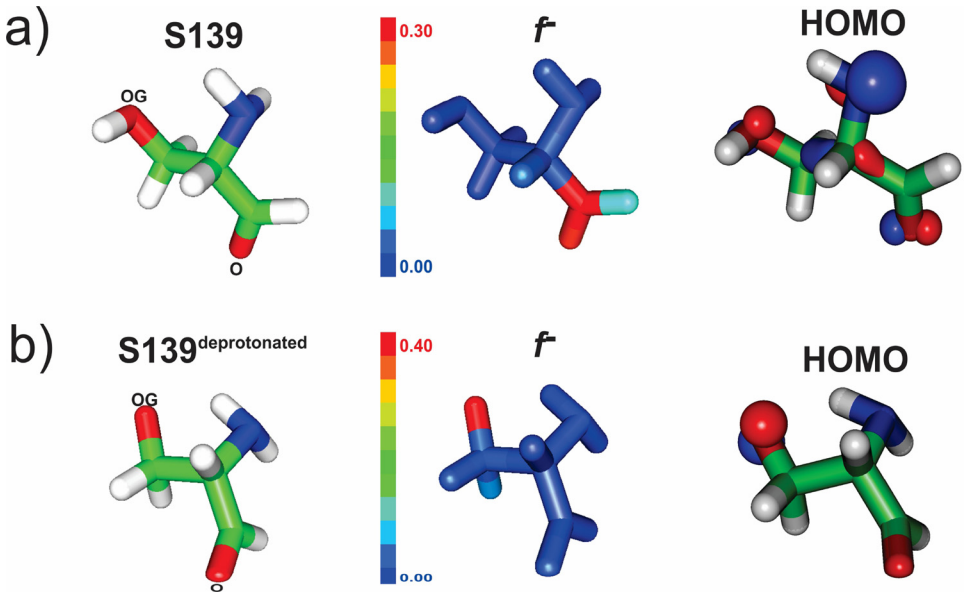

Fig. 4. Condensed-to-atoms Fukui indexes (CAFIs) and HOMO representation for S139 **(a)** and deprotonated S139 **(b)** on the OG atom. f^- colours indicate the susceptibility of each atom to suffer an electrophilic attack.

atom to an electrophilic attack when the S139 become deprotonated (Fig. 4b). The analysis of the highest occupied molecular orbital HOMO of the amino acid molecule confirmed the susceptibility of S139 to an electrophilic attack. It is possible to note the HOMO of S139 covers almost all the molecule in the natural state, while the HOMO is concentrated on the atom OG on the deprotonated S139.

These results make evident that covalent binding only occurs in the presence of deprotonated S139. In the wild-type molecule, this deprotonation process occurs due to a charge transfer between the residues H57, D81 and S139, as represented in Fig. 5a. This mechanism was previously reported for other types of serine proteases (Hedstrom, 2002). For wild-type NS3 and the Q80K and T98A mutations, the distance between the atoms of residues involved in this charge exchange mechanism was consistent among the MD simulations to promote the charge transfer ($\bar{d}_{wild} = 4.03\AA$). However, we found that the L153I substitution causes the distancing between the atoms from amino acids S139 and H57 ($\bar{d}_{L153I} = 5.72\AA$), as can be seen in Fig. 5b, which may decrease the probability of the S139 being deprotonated.

The results suggest that the L153I mutation makes the deprotonation process unfeasible and, consequently, it hampers the covalent bond formation between the receptor and ligand, conferring resistance of NS3 to this type of drug. In this way, the L153I substitution may decrease the sensibility of NS3 to boceprevir. Our hypothesis is supported by the temporal analysis of sequences found on NCBI and PDB. According to (Vivancos et al. (2018)), telaprevir and boceprevir, the first DAAs used to treat chronic HCV, were initially administered in 2011. The timeline in Fig. 6 from NCBI shows that only L153 sequences were available between 1991–2000. However, during the subsequent periods (2001–2010 and 2011–2019), the pattern is opposite, in which the number of L153I sequences decreased to approximately 2% and the number of sequences increased to approximately 98%. A similar pattern was observed in the sequences obtained from PDB. During the period between 2001–2010, most of the sequences had an L residue at position 153, and in the subsequent period, marked by the introduction of DAAs, the pattern was the opposite. Interestingly, almost all NS3 enzymes with the L153 residue found on PDB were covalently bound to its inhibitor, and this chemical interaction occurs specifically on S139. Meanwhile, almost all inhibitors of I153 proteases are not covalently bound to S139. This information was also supported by the molecular clock results (Supplementary File 1), in which the introduction of DAAs had a clear effect on the evolution of the substitution of L153 to I153.

4. Discussion

Our results revealed two mutations that may be associated with HCV resistance to boceprevir drug treatment: D168N and L153I. Our conclusions were based on the information that viral inhibition is carried out in a two-step kinetic process: the initial inhibitor–binding contact due to hydrogen bonds, followed by the stabilization of the interaction by the covalent contact in the transitional state (Howe and Venkatraman, 2013).

The D168N substitution triggered an NS3 resistance mechanism similar to the ones previously reported in the literature (Halfon and Locarnini, 2011; Meeprasert et al., 2014). This mutation interferes during the first step of the inhibitor–binding contact. Some studies have reported that the D168N substitution may be associated with drug failure in VHC treatment (Coppola et al., 2016; Jiang et al., 2013; Lontok et al., 2015), but the molecular mechanism of resistance was not previously elucidated. Interesting, other mutations in the same position (D168) have been associated with resistance to HCV inhibitory drugs (e.g., simeprevir, paritaprevir, asunaprevir and vaniprevir), such as the D168E/A/V/T/H/F/K/Y mutations (Halfon and Locarnini, 2011; Coppola et al., 2016). Thus, the D168 position is a key site for viral resistance against the action of antiretroviral drugs, in which a significant diversity of mutations may cause drug failure during treatment. In these cases, a substitution at the 168 position causes the loss of chemical contacts (hydrogen bonds) and the resulting destabilization of the NS3/substrate complex, which is considered the main molecular basis for enzymatic inhibition (Halfon and Locarnini, 2011; Prongay et al., 2007; Qiu et al., 2009). Furthermore, the results presented here could be applied to infer about HCV resistance in patients using others DAA, mainly, protease inhibitors.

In the L153I mutation, we proposed a new molecular mechanism of viral resistance. This new mechanism was related to a decrease in the deprotonation probability of OG on S139 of NS3, which can stop the second step of the boceprevir binding kinetic process. The NS3 protease domain of HCV is a chymotrypsin-like serine protease (Kim et al., 1996; Penin et al., 2004). In summary, a charge relay system is formed in which the carboxylic group of D81 forms a hydrogen bond with NE1 of H57 (Kim et al., 1996). This process increases the pK_a value of the H57 side chain from 7 to about 12, increasing its protonation susceptibility (Fersht and Sperling, 1973; Lin et al., 1998). Consequently, H57 deprotonates the hydroxyl group of the S139 side chain, and a proton

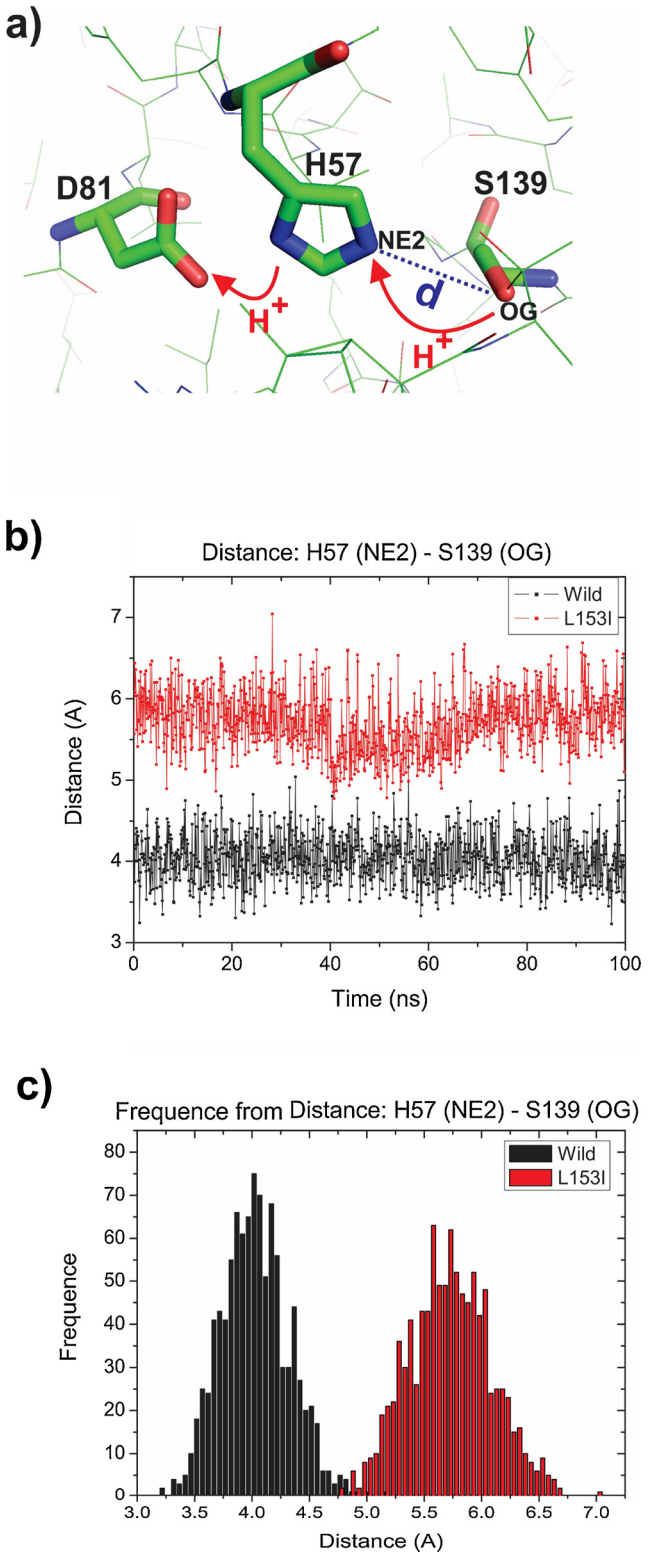

Fig. 5. (a) Schematic illustration of the S139 deprotonation process, where *d* represents the distance between the NE2 atom from residue H57 and the OG atom from residue S139. **(b)** Representation of the distance *d* between the NE2 atom and the atom OG along the MD simulations of NS3 in its wild type and L153I mutated. **(c)** Representation of the frequencies from the distance *d* values between the NE2 atom and the atom OG along the MD simulations of NS3 in its wild type and L153I mutated.

shuttles to NE2 of H57 (Hedstrom, 2002). Then, the OG from S139 mounts a nucleophilic attacks against the carbonyl carbon of the substrate's scissile bond, resulting in the formation of an oxyanion-containing tetrahedral intermediate (Hedstrom, 2002; Raney et al., 2010; Malcolm et al., 2006). At this point, protonated H57 acts as a general acid, assisting in the collapse of the tetrahedral intermediate and the cleavage of the substrate (Hedstrom, 2002; Raney et al., 2010). These three amino acid residues are known as the catalytic triad and are fundamental to the action of NS3.

Boceprevir acts by binding covalently and reversibly to the catalytic triad (Malcolm et al., 2006). Thus, our molecular dynamics simulations suggest that the presence of the L153I mutation changes the three-dimensional structure of NS3, which results in an increase of the distance between the NE2 of H57 and OG of S139. This structural alteration could impair the stability of the binding of the drug to the catalytic triad (H57, D81 and S139). This resistance model is based on intrinsic characteristics of the NS3 protein and, in this way, it can be extended to any other drug that requires covalent binding to S139 for stabilization of the complex receptor/ligand. In this context, in addition to the first generation DAAs (boceprevir and telaprevir), our resistance model can be extended to new generation drugs which covalently bond to NS3 protein, such as narlaprevir (Arasappan et al., 2010; Ashraf et al., 2019). In addition, our data suggest that this mutation has been occuring more frequently in the population after the year 2011, which coincides with the beginning of the use of boceprevir as a treatment for HCV (Vivancos et al., 2018). Thus, after the use of boceprevir, HCV *quasispecies* may have caused genetic variability, which may have impact on the use of other DAAs.

At the same time that the L153I mutation increases resistivity to inhibition to boceprevir, it could decreases the catalytic efficiency of HCV (Franco et al., 2008). In this way, some studies reported possible correlations between the catalytic efficiency of the NS3 protease and its responsiveness to DAAs (Rimmert et al., 2014; Imhof and Simmonds, 2011). Kramer et al. (Kramer et al., 2014) showed by molecular dynamical simulations that the distance between the catalytic triad residues (H57, A81 and S139) could be related to altered catalytic activity and drug susceptibility seen in NS3 proteases. These previous results support the model proposed in our study, in which also was observed that the L153I substitution causes instability (i.e., the increasing in the distance between NE2 of H57 and S139) in the catalytic triad of the NS3.

The results from the time course analysis of NS3 mutations (especially the results from the PDB) show that the drugs that covalently bind to the S139 residue were developed considering an NS3 molecular structure containing the L153 residue. This occurred because most of the crystallographic structures available in PDB during the development of DAAs such as boceprevir (2001–2010) had an L residue at position 153. However, the I153 residue is currently predominant in the NCBI and PDB both databases. Thus, nowadays HCV has low sensitivity to this type of drug, and these data could explain why boceprevir is no longer efficient in chronic hepatitis C therapy. In this way, our results may help to guide a safe and effective use of DAAs. Some studies have shown a low genetic barrier to resistance and extensive drug–drug interactions (Clark et al., 2019; González-Colominas et al., 2019). Thus, a deeper understanding about the virus-drug interactions are extremely important to develop new HCV protease inhibitors.

5. Conclusion

Two mutations were identified that may be associated with HCV resistance to boceprevir drug treatment: D168N and L153I.

The D168N substitution on NS3 induces UVR, according to a molecular resistance mechanism that was already explained in the literature, characterized by the destabilization of hydrogen bonds between the receptor and the ligand.

Our analyses also showed that the covalent binding between the

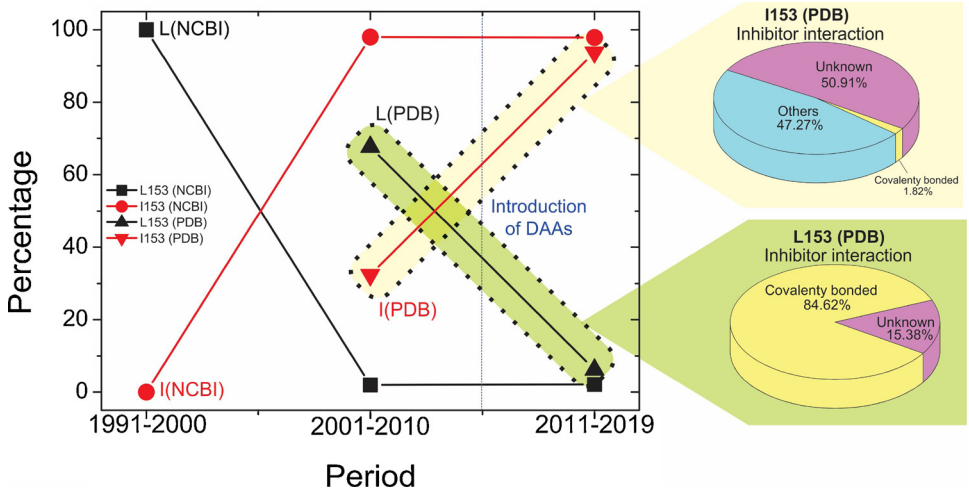

Fig. 6. Timeline of the percentage of NS3 sequences in NCBI with the L residue at 153 position. The percentage was determined by calculating the number of sequences with an L residue at position 153 out of the total number of sequences.

S139 residue of NS3 and the electrophilic trap on boceprevir is crucial for the stabilization of the inhibitor–protease and, consequently, for the drug inhibitory activity. The viability of this covalent binding is directly correlated with the probability of the S139 being deprotonated. Therefore, we found that the L153I mutation decreases the S139 deprotonation susceptibility and induces viral resistance to the drug treatment. In this sense, we propose this new mechanism of HCV resistance to explain cases of UVR in patients treated with boceprevir or any other drug which covalently binds to S139.

The data presented here could be a guide to infer about HCV *quasispecies* circulating after selective pressure of boceprevir and a model to explain resistance models to others DAAs.

Declaration of Competing Interest

None.

Acknowledgements

We acknowledge Fundação de Amparo à Pesquisa do Estado de São Paulo (FAPESP), Brazil, Grant ID: 13/21214-9. This research was also supported by resources supplied by the Center for Scientific Computing (NCC/GridUNESP) of the São Paulo State University (UNESP), Brazil.

Appendix A. Supplementary data

Supplementary data associated with this article can be found, in the online version, at https://doi.org/10.1016/j.virusres.2019.197778.

References

Ali, S.Q., Zehra, A., Naqvi, B.S., Shah, S., Bushra, R., 2010. Resistance pattern of ciprofloxacin against different pathogens. Oman Med. J. 25, 294–298. https://doi.org/10.5001/omj.2010.85.

Arasappan, A., Bennett, F., Bogen, S.L., Venkatraman, S., Blackman, M., Chen, K.X., Hendrata, S., Huang, Y., Huelgas, R.M., Nair, L., Padilla, A.I., Pan, W., Pike, R., Pinto, P., Ruan, S., Sannigrahi, M., Velazquez, F., Vibulbhan, B., Wu, W., Yang, W., Saksena, A.K., Girijavallabhan, V., Shih, N.-Y., Kong, J., Meng, T., Jin, Y., Wong, J., McNamara, P., Prongay, A., Madison, V., Piwinski, J.J., Cheng, K.-C., Morrison, R., Malcolm, B., Tong, X., Ralston, R., Njoroge, F.G., 2010. Discovery of Narlaprevir (SCH 900518): a potent, second generation HCV NS3 serine protease inhibitor. ACS Med. Chem. Lett. 1, 64–69. https://doi.org/10.1021/ml9000276.

Ashraf, M.U., Iman, K., Khalid, M.F., Salman, H.M., Shafi, T., Rafi, M., Javaid, N., Hussain, R., Ahmad, F., Shahzad-Ul-Hussan, S., Mirza, S., Shafiq, M., Afzal, S., Hamera, S., Anwar, S., Qazi, R., Idrees, M., Qureshi, S.A., Chaudhary, S.U., 2019. Evolution of efficacious pangenotypic hepatitis C virus therapies. Med. Res. Rev. 39, 1091–1136. https://doi.org/10.1002/med.21554.

Boceprevir | C27H45N5O5 | ChemSpider, (2019). http://www.chemspider.com/Chemical-Structure.8499830.html?rid=804b888d-f5d3-4873-9eaa-cccda664f353 (n.d.) (Accessed 16 November 2017).

Borgia, S.M., Hedskog, C., Parhy, B., Hyland, R.H., Stamm, L.M., Brainard, D.M., Subramanian, M.G., McHutchison, J.G., Mo, H., Svarovskaia, E., Shafran, S.D., 2018. Identification of a novel hepatitis C virus genotype from Punjab, India: expanding classification of hepatitis C virus into 8 genotypes. J. Infect. Dis. 218, 1722–1729. https://doi.org/10.1093/infdis/jiy401.

Brooks, B.R., Brooks, C.L., MacKerell, A.D., Nilsson, L., Petrella, R.J., Roux, B., Won, Y., Archontis, G., Bartels, C., Boresch, S., Caflisch, A., Caves, L., Cui, Q., Dinner, A.R., Feig, M., Fischer, S., Gao, J., Hodoscek, M., Im, W., Kuczera, K., Lazaridis, T., Ma, J., Ovchinnikov, V., Paci, E., Pastor, R.W., Post, C.B., Pu, J.Z., Schaefer, M., Tidor, B., Venable, R.M., Woodcock, H.L., Wu, X., Yang, W., York, D.M., Karplus, M., 2009. CHARMM: the biomolecular simulation program. J. Comput. Chem. 30, 1545–1614. https://doi.org/10.1002/jcc.21287.

Cesarino, I., Plana Simões, R., Carlos Lavarda, F., Batagin-Neto, A., 2016. Electrochemical Oxidation of Sulfamethazine on a Glassy Carbon Electrode Modified with Graphene and Gold Nanoparticles. https://doi.org/10.1016/j.electacta.2016.01.178.

V.C. Clark, J.A. Peter, D.R. Nelson, New therapeutic strategies in HCV: second-generation protease inhibitors, Liver Int.. 33 (n.d.) 80–84. doi:10.1111/liv.12061.

Coppola, N., Minichini, C., Starace, M., Sagnelli, C., Sagnelli, E., 2016. Clinical impact of the hepatitis C virus mutations in the era of directly acting antivirals. J. Med. Virol. 88, 1659–1671. https://doi.org/10.1002/jmv.24527.

Cuypers, L., Libin, P., Schrooten, Y., Theys, K., Di Maio, V.C., Cento, V., Lunar, M.M., Nevens, F., Poljak, M., Ceccherini-Silberstein, F., Nowé, A., Van Laethem, K., Vandamme, A.-M., 2017. Exploring resistance pathways for first-generation NS3/4A protease inhibitors boceprevir and telaprevir using Bayesian network learning. Infect. Genet. Evol. J. Mol. Epidemiol. Evol. Genet. Infect. Dis. 53, 15–23. https://doi.org/10.1016/j.meegid.2017.05.007.

Delport, W., Poon, A.F.Y., Frost, S.D.W., Kosakovsky Pond, S.L., 2010. Datamonkey 2010: a suite of phylogenetic analysis tools for evolutionary biology. Bioinformatics 26, 2455–2457. https://doi.org/10.1093/bioinformatics/btq429.

Dolinsky, T.J., Nielsen, J.E., McCammon, J.A., Baker, N.A., 2004. PDB2PQR: an automated pipeline for the setup of Poisson-Boltzmann electrostatics calculations. Nucleic Acids Res. 32, W665–667. https://doi.org/10.1093/nar/gkh381.

Donini, C.A., da Silva, M.K.L., Simões, R.P., Cesarino, I., 2018. Reduced graphene oxide modified with silver nanoparticles for the electrochemical detection of estriol. J. Electroanal. Chem. 809, 67–73. https://doi.org/10.1016/j.jelechem.2017.12.054.

Drummond, A.J., Suchard, M.A., Xie, D., Rambaut, A., 2012. Bayesian Phylogenetics with BEAUti and the BEAST 1.7. Mol. Biol. Evol. 29, 1969–1973. https://doi.org/10.1093/molbev/mss075.

Edgar, R.C., 2004. MUSCLE: multiple sequence alignment with high accuracy and high throughput. Nucleic Acids Res. 32, 1792–1797. https://doi.org/10.1093/nar/gkh340.

Fersht, A.R., Sperling, J., 1973. The charge relay system in chymotrypsin and chymotrypsinogen. J. Mol. Biol. 74, 137–149.

Foloppe, N., Sagemark, J., Nordstrand, K., Berndt, K.D., Nilsson, L., 2001. Structure, dynamics and electrostatics of the active site of glutaredoxin 3 from Escherichia coli: comparison with functionally related proteins. J. Mol. Biol. 310, 449–470. https://doi.org/10.1006/jmbi.2001.4767.

Franco, S., Clotet, B., Martínez, M.A., 2008. A wide range of NS3/4A protease catalytic efficiencies in HCV-infected individuals. Virus Res. 131, 260–270. https://doi.org/10.1016/j.virusres.2007.10.003.

Frisch, M.J., Trucks, G.W., Schlegel, H.B., Scuseria, G.E., Robb, M.A., Cheeseman, J.R., 2016. Gaussian 16, Wallingford, CT.

Frost, S.D.W., Magalis, B.R., Kosakovsky Pond, S.L., 2018. Neutral theory and rapidly evolving viral pathogens. Mol. Biol. Evol. 35, 1348–1354. https://doi.org/10.1093/molbev/msy088.

E. González-Colominas, T. Broquetas, A. Retamero, M. García-Retortillo, N. Cañete, S.

Coll, R. Pellicer, M.D. Giménez, B. Cabrero, F. Bory, H. Knobel, E. Salas, R. Solà, J.A. Carrión, Drug–drug interactions of telaprevir and boceprevir in HCV-monoinfected and HIV/HCV-coinfected patients can modify the adherence, Liver Int.. 35 (n.d.) 1557–1565. doi:https://doi.org/10.1111/liv.12729.

Halfon, P., Locarnini, S., 2011. Hepatitis C virus resistance to protease inhibitors. J. Hepatol. 55, 192–206. https://doi.org/10.1016/j.jhep.2011.01.011.

Han, J., Pei, J., Kamber, M., 2011. Data Mining: Concepts and Techniques. Elsevier.

Hedstrom, L., 2002. Serine protease mechanism and specificity. Chem. Rev. 102, 4501–4524.

Howe, A.Y.M., Venkatraman, S., 2013. The discovery and development of boceprevir: a novel, first-generation inhibitor of the hepatitis C virus NS3/4A serine protease. J. Clin. Transl. Hepatol. 1, 22–32. https://doi.org/10.14218/JCTH.2013.002XX.

Huang, Y., Niu, B., Gao, Y., Fu, L., Li, W., 2010. CD-HIT Suite: a web server for clustering and comparing biological sequences. Bioinforma. Oxf. Engl. 26, 680–682. https://doi.org/10.1093/bioinformatics/btq003.

Imhof, I., Simmonds, P., 2011. Genotype differences in susceptibility and resistance development of hepatitis C virus to protease inhibitors telaprevir (VX-950) and danoprevir (ITMN-191). Hepatol. Baltim. Md. 53, 1090–1099. https://doi.org/10.1002/hep.24172.

Jiang, M., Mani, N., Lin, C., Ardzinski, A., Nelson, M., Reagan, D., Bartels, D., Zhou, Y., Nicolas, O., Rao, B.G., Müh, U., Hanzelka, B., Tigges, A., Rijnbrand, R., Kieffer, T.L., 2013. In vitro phenotypic characterization of hepatitis C virus NS3 protease variants observed in clinical studies of telaprevir. Antimicrob. Agents Chemother. 57, 6236–6245. https://doi.org/10.1128/AAC.01578-13.

Kim, J.L., Morgenstern, K.A., Lin, C., Fox, T., Dwyer, M.D., Landro, J.A., Chambers, S.P., Markland, W., Lepre, C.A., O'Malley, E.T., Harbeson, S.L., Rice, C.M., Murcko, M.A., Caron, P.R., Thomson, J.A., 1996. Crystal structure of the hepatitis C virus NS3 protease domain complexed with a synthetic NS4A cofactor peptide. Cell 87, 343–355.

Kramer, M., Halleran, D., Rahman, M., Iqbal, M., Anwar, M.I., Sabet, S., Ackad, E., Yousef, M., 2014. Comparative molecular dynamics simulation of hepatitis C virus NS3/4A protease (genotypes 1b, 3a and 4a) predicts conformational instability of the catalytic triad in drug resistant strains. PLoS One 9, e104425. https://doi.org/10.1371/journal.pone.0104425.

Lin, J., Cassidy, C.S., Frey, P.A., 1998. Correlations of the basicity of his 57 with transition state analogue binding, substrate reactivity, and the strength of the low-barrier hydrogen bond in chymotrypsin. Biochemistry 37, 11940–11948. https://doi.org/10.1021/bi980278s.

Lontok, E., Harrington, P., Howe, A., Kieffer, T., Lennerstrand, J., Lenz, O., McPhee, F., Mo, H., Parkin, N., Pilot-Matias, T., Miller, V., 2015. Hepatitis C virus drug resistance-associated substitutions: state of the art summary. Hepatol. Baltim. Md. 62, 1623–1632. https://doi.org/10.1002/hep.27934.

Malcolm, B.A., Liu, R., Lahser, F., Agrawal, S., Belanger, B., Butkiewicz, N., Chase, R., Gheyas, F., Hart, A., Hesk, D., Ingravallo, P., Jiang, C., Kong, R., Lu, J., Pichardo, J., Prongay, A., Skelton, A., Tong, X., Venkatraman, S., Xia, E., Girijavallabhan, V., Njoroge, F.G., 2006. SCH 503034, a mechanism-based inhibitor of hepatitis C virus NS3 protease, suppresses polyprotein maturation and enhances the antiviral activity of alpha interferon in replicon cells. Antimicrob. Agents Chemother. 50, 1013–1020. https://doi.org/10.1128/AAC.50.3.1013-1020.2006.

Meeprasert, A., Hannongbua, S., Rungrotmongkol, T., 2014. Key binding and susceptibility of NS3/4A serine protease inhibitors against hepatitis C virus. J. Chem. Inf. Model. 54, 1208–1217. https://doi.org/10.1021/ci400605a.

Miller, M.A., Pfeiffer, W., Schwartz, T., 2010. Creating the CIPRES Science Gateway for inference of large phylogenetic trees. 2010 Gatew. Comput. Environ. Workshop GCE 1–8. https://doi.org/10.1109/GCE.2010.5676129.

Morales, J.M., Aguado, J.M., 2012. Hepatitis C and renal transplantation. Curr. Opin. Organ Transplant. 17, 609–615. https://doi.org/10.1097/MOT.0b013e32835a2bac.

Penin, F., Dubuisson, J., Rey, F.A., Moradpour, D., Pawlotsky, J.-M., 2004. Structural biology of hepatitis C virus. Hepatology 39, 5–19. https://doi.org/10.1002/hep.20032.

Prongay, A.J., Guo, Z., Yao, N., Pichardo, J., Fischmann, T., Strickland, C., Myers, J., Weber, P.C., Beyer, B.M., Ingram, R., Hong, Z., Prosise, W.W., Ramanathan, L., Taremi, S.S., Yarosh-Tomaine, T., Zhang, R., Senior, M., Yang, R.-S., Malcolm, B., Arasappan, A., Bennett, F., Bogen, S.L., Chen, K., Jao, E., Liu, Y.-T., Lovey, R.G., Saksena, A.K., Venkatraman, S., Girijavallabhan, V., Njoroge, F.G., Madison, V., 2007. Discovery of the HCV NS3/4A protease inhibitor (1R,5S)-N-[3-amino-1-(cyclobutylmethyl)-2,3-dioxopropyl]-3- [2(S)-[[[(1,1-dimethylethyl)amino]carbonyl] amino]-3,3-dimethyl-1-oxobutyl]- 6,6-dimethyl-3-azabicyclo[3.1.0]hexan-2(S)-carboxamide (Sch 503034) II. Key steps in structure-based optimization. J. Med. Chem. 50, 2310–2318. https://doi.org/10.1021/jm060173k.

Qiu, P., Sanfiorenzo, V., Curry, S., Guo, Z., Liu, S., Skelton, A., Xia, E., Cullen, C., Ralston, R., Greene, J., Tong, X., 2009. Identification of HCV protease inhibitor resistance mutations by selection pressure-based method. Nucleic Acids Res. 37, e74. https://doi.org/10.1093/nar/gkp251.

Raney, K.D., Sharma, S.D., Moustafa, I.M., Cameron, C.E., 2010. Hepatitis C virus non-structural protein 3 (HCV NS3): a multifunctional antiviral target. J. Biol. Chem. 285, 22725–22731. https://doi.org/10.1074/jbc.R110.125294.

Rimmert, B., Sabet, S., Ackad, E., Yousef, M.S., 2014. A 3D structural model and dynamics of hepatitis C virus NS3/4A protease (genotype 4a, strain ED43) suggest conformational instability of the catalytic triad: implications in catalysis and drug resistivity. J. Biomol. Struct. Dyn. 32, 950–958. https://doi.org/10.1080/07391102.2013.800001.

Sanjuán, R., Domingo-Calap, P., 2016. Mechanisms of viral mutation. Cell. Mol. Life Sci. CMLS 73, 4433–4448. https://doi.org/10.1007/s00018-016-2299-6.

Shen, C., Yu, X., Harrison, R.W., Weber, I.T., 2016. Automated prediction of HIV drug resistance from genotype data. BMC Bioinformatics 17. https://doi.org/10.1186/s12859-016-1114-6.

Shiryaev, S.A., Cheltsov, A.V., Strongin, A.Y., 2012. Probing of exosites leads to novel inhibitor scaffolds of HCV NS3/4A proteinase. PLoS One 7. https://doi.org/10.1371/journal.pone.0040029.

Sievers, F., Higgins, D.G., 2014. Clustal Omega, accurate alignment of very large numbers of sequences. Methods Mol. Biol. Clifton NJ. 1079, 105–116. https://doi.org/10.1007/978-1-62703-646-7_6.

Simmonds, P., Bukh, J., Combet, C., Deléage, G., Enomoto, N., Feinstone, S., Halfon, P., Inchauspé, G., Kuiken, C., Maertens, G., Mizokami, M., Murphy, D.G., Okamoto, H., Pawlotsky, J.-M., Penin, F., Sablon, E., Shin-I, T., Stuyver, L.J., Thiel, H.-J., Viazov, S., Weiner, A.J., Widell, A., 2005. Consensus proposals for a unified system of nomenclature of hepatitis C virus genotypes. Hepatol. Baltim. Md. 42, 962–973. https://doi.org/10.1002/hep.20819.

Smith, D.B., Bukh, J., Kuiken, C., Muerhoff, A.S., Rice, C.M., Stapleton, J.T., Simmonds, P., 2014. Expanded classification of hepatitis C virus into 7 genotypes and 67 subtypes: updated criteria and genotype assignment web resource. Hepatol. Baltim. Md. 59, 318–327. https://doi.org/10.1002/hep.26744.

Stamatakis, A., 2014. RAxML version 8: a tool for phylogenetic analysis and post-analysis of large phylogenies. Bioinformatics 30, 1312–1313. https://doi.org/10.1093/bioinformatics/btu033.

Vanommeslaeghe, K., Hatcher, E., Acharya, C., Kundu, S., Zhong, S., Shim, J., Darian, E., Guvench, O., Lopes, P., Vorobyov, I., Mackerell, A.D., 2010. CHARMM general force field: a force field for drug-like molecules compatible with the CHARMM all-atom additive biological force fields. J. Comput. Chem. 31, 671–690. https://doi.org/10.1002/jcc.21367.

Venkatraman, S., 2012. Discovery of boceprevir, a direct-acting NS3/4A protease inhibitor for treatment of chronic hepatitis C infections. Trends Pharmacol. Sci. 33, 289–294. https://doi.org/10.1016/j.tips.2012.03.012.

Vivancos, M.J., Moreno, A., Quereda, C., 2018. Treatment of hepatitisC virus with direct-acting antivirals: practical aspects and current situation. Rev. Clin. Esp. 218, 29–37. https://doi.org/10.1016/j.rce.2017.07.006.